

An integrated study of urban microclimates in Chongqing, China: Historical weather data, transverse measurement and numerical simulation



Runming Yao^{a,*}, Qing Luo^b, Zhiwen Luo^a, Lai Jiang^a, Yu Yang^b

^a School of Construction Management and Engineering, University of Reading, United Kingdom

^b Key Laboratory of the Three Gorges Reservoir Region's Eco-Environment under the Ministry of Education, Chongqing University, PR China

ARTICLE INFO

Article history:

Available online 30 September 2014

Keywords:

Urban microclimate
Chongqing
Urbanization
Field measurement
Mobile transverse
Urban heat island

ABSTRACT

Chongqing is the largest central-government-controlled municipality in China, which is now undergoing a rapid urbanization. The question remains open: What are the consequences of such rapid urbanization in Chongqing in terms of urban microclimates? An integrated study comprising three different research approaches is adopted in the present paper. By analyzing the observed annual climate data, an average rising trend of 0.10 °C/decade was found for the annual mean temperature from 1951 to 2010 in Chongqing, indicating a higher degree of urban warming in Chongqing. In addition, two complementary types of field measurements were conducted: fixed weather stations and mobile transverse measurement. Numerical simulations using a house-developed program are able to predict the urban air temperature in Chongqing. The urban heat island intensity in Chongqing is stronger in summer compared to autumn and winter. The maximum urban heat island intensity occurs at around midnight, and can be as high as 2.5 °C. In the daytime, an urban cool island exists. Local greenery has a great impact on the local thermal environment. Urban green spaces can reduce urban air temperature and therefore mitigate the urban heat island. The cooling effect of an urban river is limited in Chongqing, as both sides of the river are the most developed areas, but the relative humidity is much higher near the river compared with the places far from it.

© 2014 Published by Elsevier Ltd.

1. Introduction

The proportion of the global population in urban areas has increased conspicuously from 29% in 1950 to 49% in 2005, and urbanization is projected to increase even further to 60% in 2030 (NU, 2005). There is a much higher urbanization rate and total population in developing countries, but China is among the highest. China now has 89 cities with a population of a million or more compared to 32 in India and 37 in the United States. The government estimates that 44% of China's population lives in cities, this figure will be 60% by 2020 (Normile, 2008).

This rapid urbanization brings about a series of environmental consequences. In one way, cities strongly contribute to the greenhouse gases emissions and consequently to global warming (IPCC, 2007). It is reported that cities are responsible for 75% of global energy consumption and 80% of greenhouse gas emissions (Ash, Jasny, Roberts, Stone, & Sugden, 2008). And they create a district

urban climate at the city scale (Grimmond, 2007). An urban climate differs from its rural counterpart in its unique underlying surface characteristics and the anthropogenic activities within it (Oke, 1988). Urban infrastructures, together with changes to the morphology and materials of the surface, alter the energy and water exchange between surfaces and the adjacent atmosphere, as well as the airflows (Belcher, 2005). In the coming decades, the complex interaction between the effects of global change at a regional scale and the evolution of cities themselves will probably lead to a deep change of urban climate. A better scientific understanding of urban environmental physics can help optimize urban planning to achieve a sustainable city development (Bowler, Buyung-Ali, Knight, & Pullin, 2010; Mills, 2007) and seek useful mitigation solutions to fight against climate change.

Urban climate is characterized by a higher temperature, lower humidity, and weaker winds than surrounding rural areas. The first urban climate study was carried out by Luke Howard in London. He found that the night in the city of London was 3.7 °C warmer than in the countryside in the early 1800s (Howard, 1833). Since then, many studies have attempted to address the impact of urbanization on the urban microclimate in other different cities worldwide

* Corresponding author.

E-mail address: r.yao@reading.ac.uk (R. Yao).

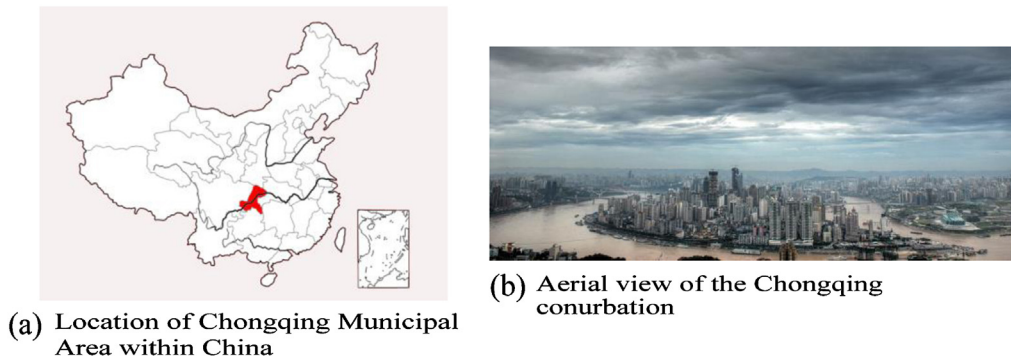


Fig. 1. Location and morphology of Chongqing City.

such as New York City (Bornstein, 1968), Cairo (Robaa, 2013), South Africa (Kruger and Shongwe, 2004), East China (Si, Ren, Liang, & Lin, 2012; Wong & Yu, 2005), and a medium-sized Mediterranean city (Busato, Lazzarin, & Noro, 2014; Papanastasiou & Kittas, 2012). We also reviewed most relevant studies for cities with a similar climate to Chongqing, i.e., a mild climate but with hot summers and cold winters. Huang, Li, Zhao, and Zhu (2008) examined the impacts of different ground covers on the urban heat island in Nanjing, China during the summer period. Their results showed that bare concrete cover had the highest daytime air temperature, while the woods or the shade of trees had the lowest. Strong urban heat island (UHI) effects occurred around midnight. However, comparison between different seasons was not possible since measurements were only made in summer. However, Zeng, Qiu, Gu, He, and Wang (2009) identified the seasonal pattern of the UHI in Nanjing from 1961 to 2005 based on four meteorological stations in Nanjing. Temperatures were highest in summer and lowest in winter and the average UHI intensity was about 0.5°C . The annual increasing rate of mean air temperature was $0.109^{\circ}\text{C}/10\text{a}$. In Shanghai, the spatiotemporal patterns of UHI were quantitatively examined for the years 1997

and 2008 using remote sensing and GIS. The unprecedented land use/land cover (LULC) change and population shift from 1997 to 2008 had resulted in an expanding UHI effect both in the extent and magnitude (Zhang et al., 2013). Locally, Yang, Lau, and Qian (2010) investigated the relationship of building layout and density with the summer time UHI in high-rise areas in Shanghai. They found that the day-time UHI was closely related to the site shading factor, while the night-time UHI was more influenced by local anthropogenic heat. Likewise, a study in Wuhan also indicated that land-use patterns had significant impacts on the UHI, and forest and cropland can effectively mitigate the UHI in Wuhan due to its large spatial extent and homogeneous spatial distribution (Wu, Ye, Shi, and Clarke, 2014).

However, Chongqing is very different from the above-mentioned cities due to its very complex geographical settings, though it shares a similar climate. Chongqing has a land area of $82,401\text{km}^2$, of which 42% could be classified as urban. It is located in the southwest part of China on the southeast edge of the Sichuan Basin between the Tibetan Plateau and the Yangtze Plain, as shown in Fig. 1. It is adjacent to Hubei, Hunan, Shaanxi,



Fig. 2. Distribution of weather stations in Chongqing (Zhang et al., 2009).

Sichuan and Guizhou provinces. The upstream area of the Yangtze River intersects the city. The Jialing and Wujiang Rivers join the Yangtze River from the north and the south respectively in this area. The city is generally surrounded by the Daba Mountain, the Wu Mountain, the Wulin Mountain and the Dalou Mountain. The main terrains of Chongqing are hilly and mountainous with many sloping fields. No international peer-reviewed research on Chongqing has been published, to the best of our knowledge. What is more, Chongqing is now undergoing a rapid urbanization. The urbanization rate increased from 35.6% in 2000 to 48.3% in 2007, and it is estimated to reach at least 70% by 2020. The question remains open: What is the urban microclimate in Chongqing under such a unique surrounding environment? What are the consequences of such

rapid urbanization in Chongqing in terms of urban microclimates? The present paper is devoted to providing an integrated study to answer the above questions. Three types of research methods are employed. Annual microclimate trends will be firstly identified based on the data collected in government-controlled weather stations in Chongqing from 1951 to 2010. In addition, two complementary types of field measurements (fixed weather stations and mobile transverse measurement) are carried out to investigate the spatial difference of urban micro-climate parameters. Finally, a numerical simulation of the urban heat island in Chongqing using our house-developed program is presented.

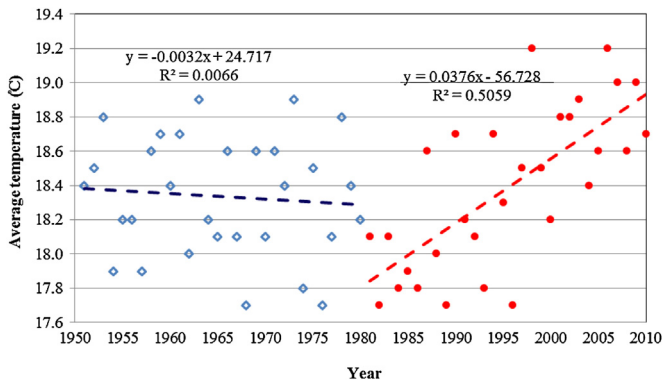


Fig. 3. Annual average temperature trend in Chongqing.

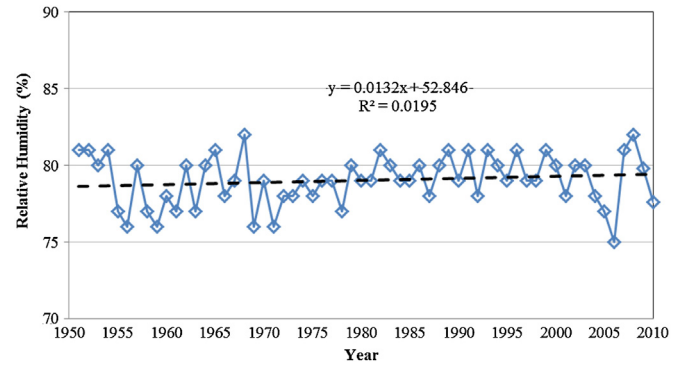


Fig. 5. Yearly variation of RH in Chongqing.

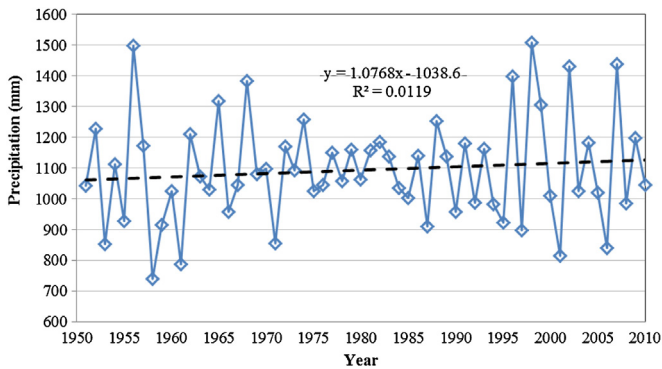


Fig. 4. Yearly variation of precipitation in Chongqing.

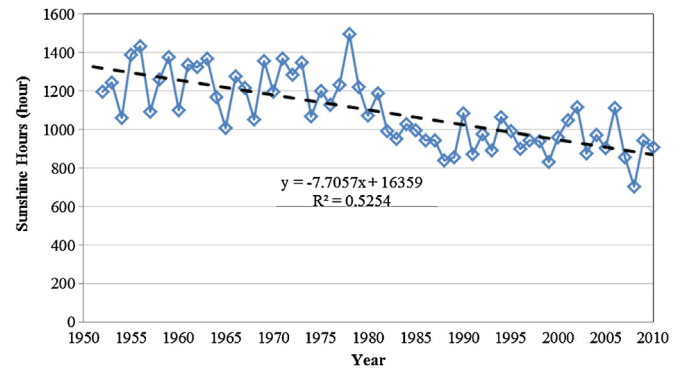


Fig. 6. Yearly variation of sunshine hours.

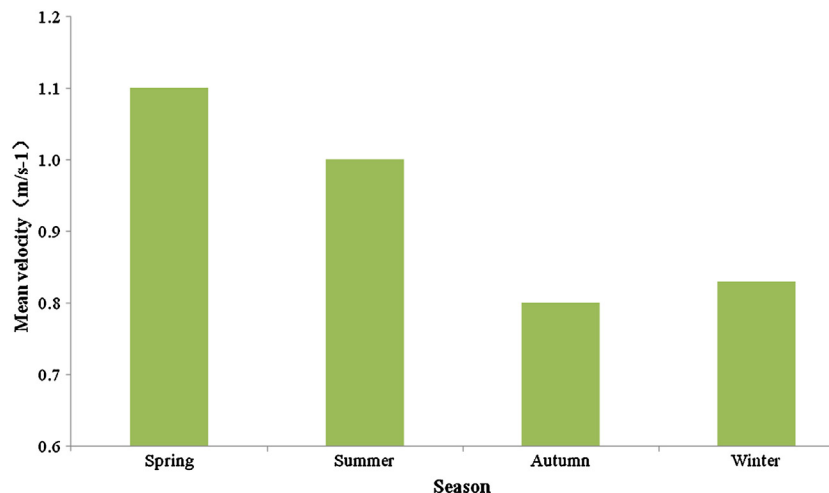


Fig. 7. Seasonal variation of mean wind speed in Chongqing (Li et al., 2010).

2. Annual trends for urban microclimates in Chongqing

The Chongqing government has operated 35 weather stations to monitor the local climate, as shown in Fig. 2. The major recorded climate parameters are air temperature, relative humidity (RH), precipitation, and wind speed. The earliest record dates back to 1951. The Chongqing Government collects and compiles all the data and publishes them annually as a statistics book (Chongqing Bureau, 2011).

2.1. Urban air temperature

According to IPCC (2007) the global mean temperature (T_{mean}), averaged over land and ocean surfaces, increased by $0.76^{\circ}\text{C} \pm 0.19^{\circ}\text{C}$ from 1850 to 1899, and $0.74^{\circ}\text{C} \pm 0.18^{\circ}\text{C}$ over the 100 years 1906–2005. This rising trend in temperature is one of the major indications of global warming and climate change. Zhang, Cheng, and Liu (2009) analyzed the data from 1961 to 2007, and found an average rising trend of $0.12^{\circ}\text{C}/\text{decade}$ for the annual T_{mean} . We extended this data from 1951 to the more recent year of 2010, and the results show a rising trend of $0.10^{\circ}\text{C}/\text{decade}$. This number is much higher than the global rising trend of $0.074^{\circ}\text{C}/\text{decade}$, indicating a higher degree of urban warming in Chongqing. The data can be further divided into two periods: before 1980 and after 1980. This rising trend is especially significant after 1980, $0.38^{\circ}\text{C}/\text{decade}$ from 1980 to 2010, with $0.62^{\circ}\text{C}/\text{decade}$ for spring

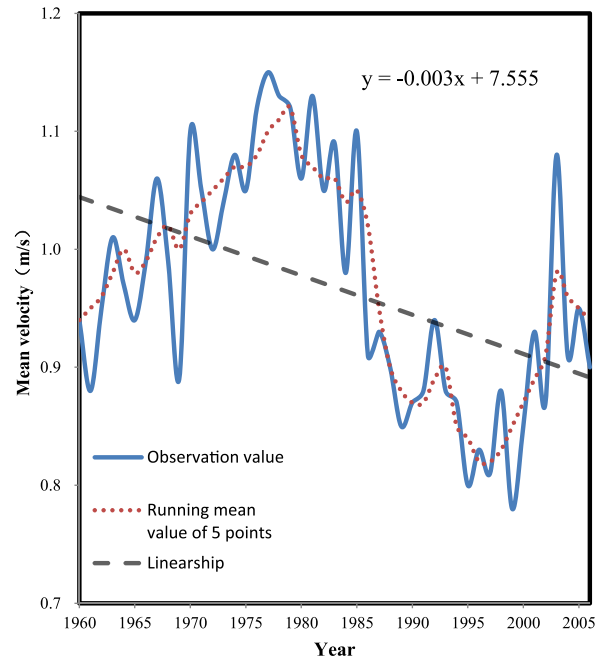
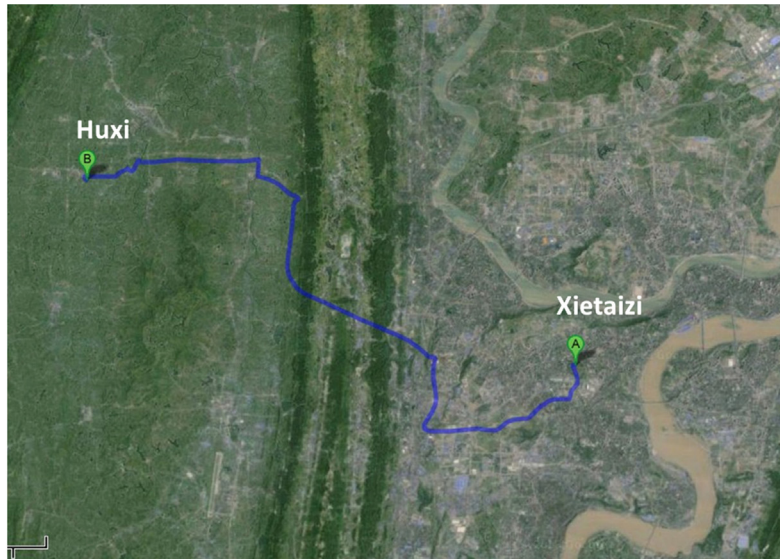


Fig. 8. Yearly variation of mean wind speed in Chongqing (Li et al., 2010).



a) Locations of Huxi and Xietaizi



b) Local environment of Huxi



c) Local environment of Xietaizi

Fig. 9. Fixed weather stations in the Chongqing area.

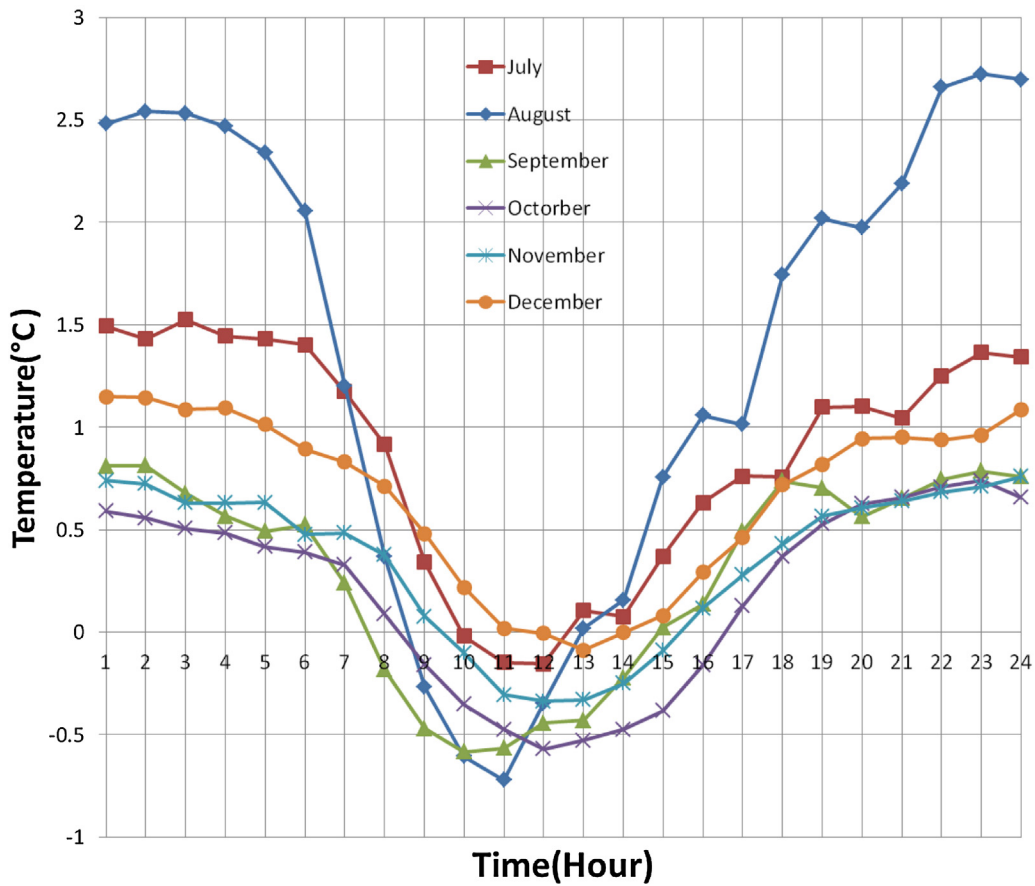


Fig. 10. Urban heat island intensity between Xietaizi and Huxi.

and $0.61\text{ }^{\circ}\text{C}/\text{decade}$ for summer. This may be attributable to the rapid urbanization in Chongqing. It is reported that the urbanization rate in Chongqing increased from 17.4% in 1990 to 53.0% in 2010, and energy consumption increased almost 10 times from 1980 to 2010 (Chongqing Bureau, 2007). All these significant changes contribute to the dramatic rising trend of urban air temperature after 1980. Interestingly, there was a decreasing trend

of $-0.032\text{ }^{\circ}\text{C}/\text{decade}$ during 1951–1980 (especially in summer, $-0.043\text{ }^{\circ}\text{C}/\text{decade}$ and spring, $-0.043\text{ }^{\circ}\text{C}/\text{decade}$). Zhao, Sun, and Cheng (2008) argued that there was a distinctly different synoptic 100 hpa circulation over the Sichuan basin during the 1960s compared to the 1980s, which contributed to a higher air temperature in summer in the 1960s. Therefore the average temperature was higher in the 1960s compared with that in the 1980s (Fig. 3).

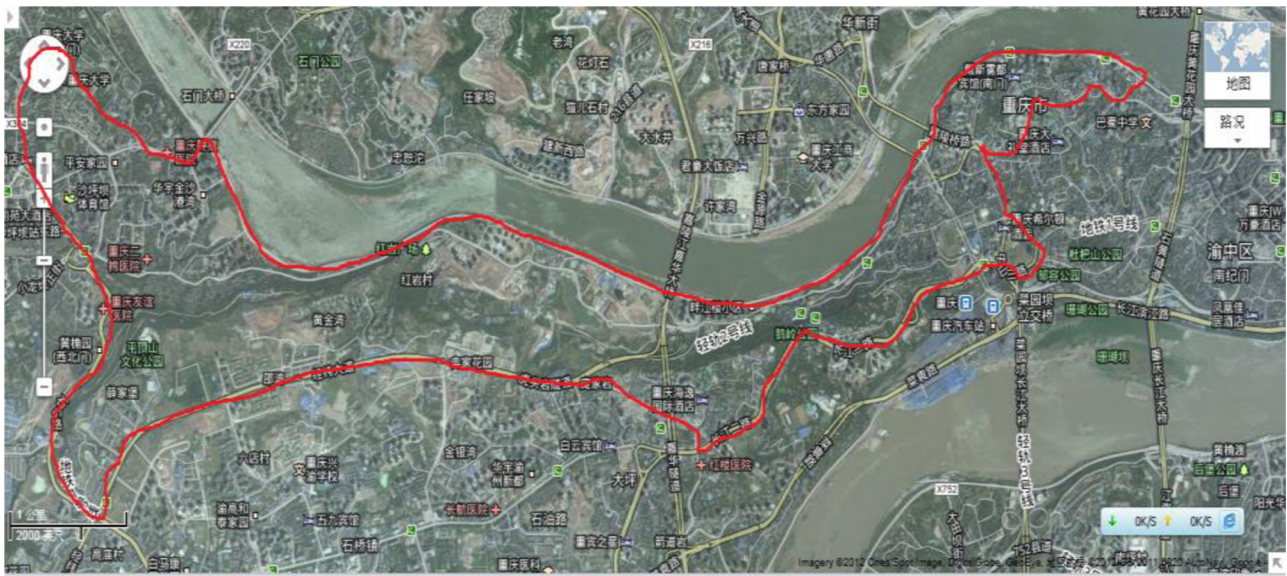


Fig. 11. Mobile transverse route.

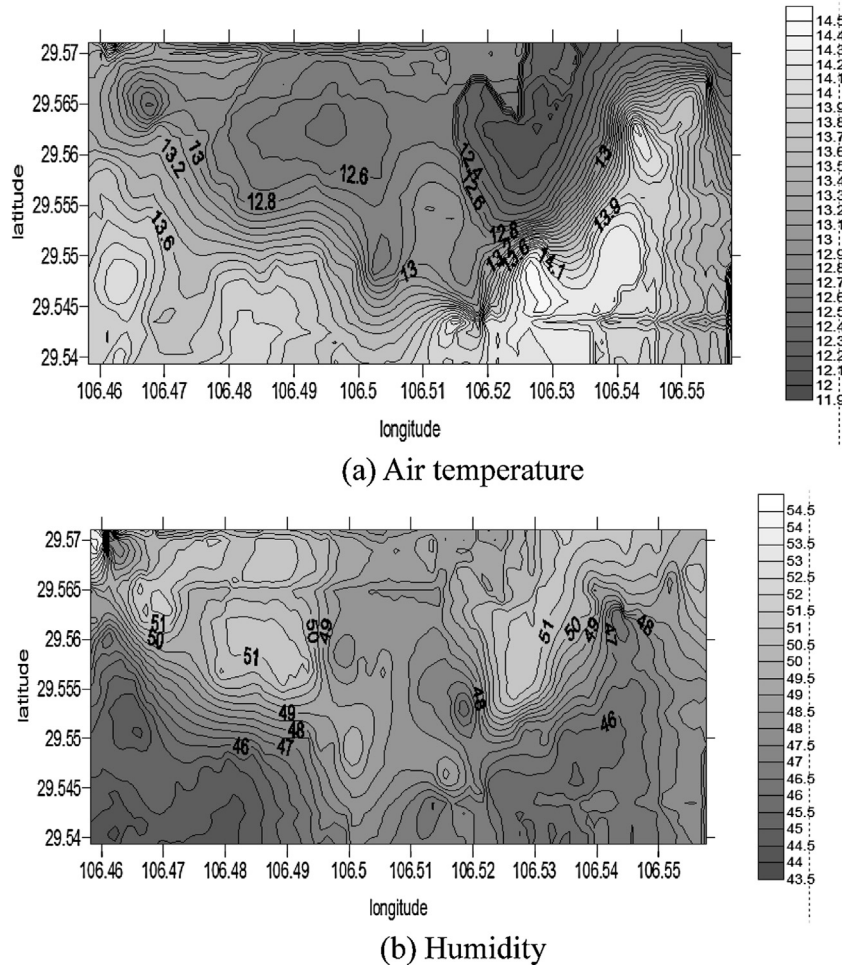


Fig. 12. Air temperature and humidity mapping for the mobile transverse route.

2.2. Urban precipitation and RH

We used the statistical data to obtain the yearly variation of precipitation and relative humidity (RH) in Chongqing (Chongqing Bureau, 2011). A slight, though not statistically significant, increase of precipitation is observed in Chongqing over almost 60 years, see Fig. 4. Many studies have revealed that the rapid urbanization is responsible for the increased amount of precipitation within the city (Mölders and Olson, 2004). The enhanced urban heat island circulation due to urbanization lifts the air mass over the city, and the higher level of human-induced aerosols contained in this rising urban air mass leads in turn to an increase in the number of condensation nuclei in the atmosphere. Therefore, more precipitation is expected within and downwind of the urban city. Another reason for the increase in precipitation is probably the influence of the Three Gorges Dam (TGD). Wu, Zhang, and Jiang (2006) found that the land-use change associated with the TGD construction has increased the precipitation in the region between Daba and Qinling Mountains after the TGD water level rose from 66 to 135 m. In accordance with precipitation, the yearly averaged RH in Chongqing is also increasing, as shown in Fig. 5. This may be also partly due to the increasing moisture released by human activities and partly due to the increased precipitation.

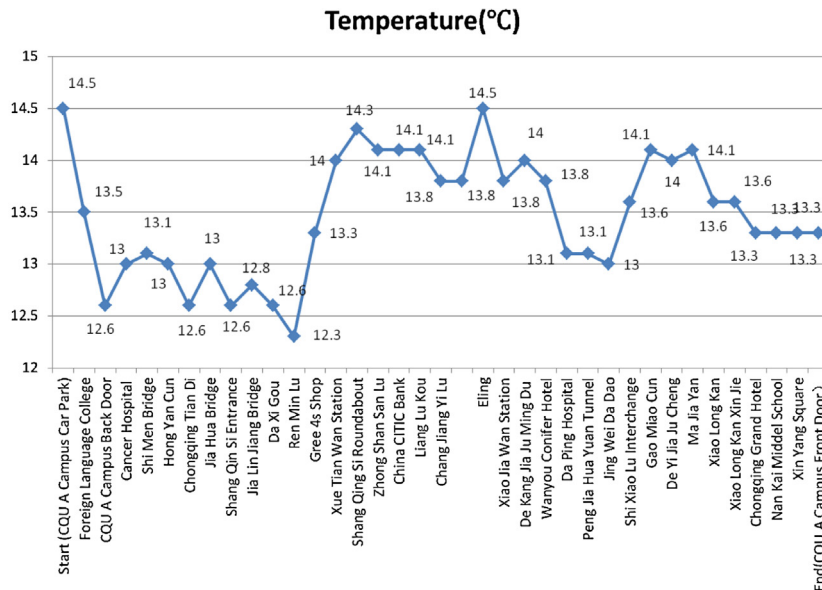
2.3. Sunshine hours

Fig. 6 shows the yearly variations in sunshine hours in Chongqing from 1951 to 2010. The sunshine hours decrease

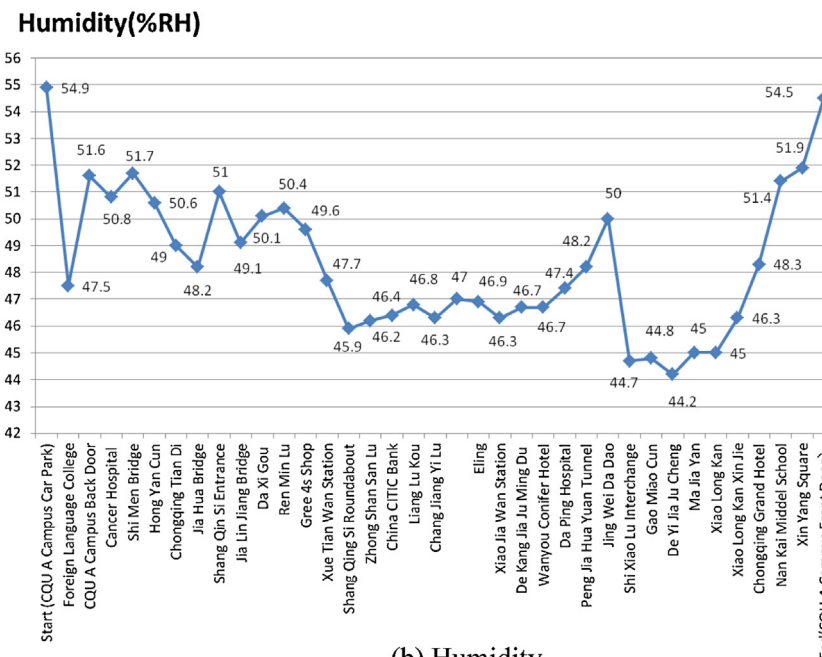
with time, especially there is a significant drop since 1980. This may be explained by the increasing levels of pollution in Chongqing. With higher levels of pollutants in air, fewer sunshine hours would be expected. This trend correlates reasonably with the average air temperature in Chongqing, i.e., a lower air temperature is expected during a period of fewer sunshine hours. However, many other factors also contribute to this.

2.4. Urban wind speed

The urban wind speed in Chongqing has changed profoundly over the past 50 years, characterized by a higher wind speed in spring and summer, but a lower value in autumn and winter, see Fig. 7. As depicted in Fig. 8, the wind speed increased till a maximum value of 1.15 m/s in 1976, and declined significantly to a minimum value of 0.8 m/s in 2000, and finally gradually increased again (Li, Geng, Dong, & Zhu, 2010). The wind speed data were collected and averaged over 34 weather stations across the urban of Chongqing City. Two possible reasons are attributable to the change, one is the change of large-scale global circulation, and the other is the change of local-scale circulation especially due to urbanization. The dramatic decrease of wind speed in Chongqing after 1970 is in accordance with the rapid urbanization taking place since 1970. Spatially, a higher wind speed is expected in the north-east and southwest parts, compared to a lower wind speed in the middle.



(a) Air temperature



(b) Humidity

Fig. 13. Air temperature and humidity at typical mobile points.

3. Field measurement

A field campaign to measure the urban thermal environment in the Chongqing area was conducted during June 2012–January 2013. This field campaign consisted of two types of measurements: fixed station measurements and mobile transverse measurements. Fixed stations can be used for long-term measurements, while mobile transverse measurements can give a full picture of the detailed, spatial distribution of temperature.

3.1. Fixed station measurements

Two fixed stations were set up for the field campaign: Huxi and Xietaizi, see Fig. 9(a). The selection of the weather stations is based on two principles: (1) local environment, i.e., urban or rural; (2) distance to the Three Gorge Reservoir (TGR). Xietaizi is close to the

area surrounding the TGR, with a distance to the TGR of 2000 m. Huxi is 14 Km from the TGR region. This makes it possible to compare the different locations with different distances from the TGR region. The local environmental conditions surrounding the two measuring stations are depicted in Fig. 9(b and c). Huxi used to be an agricultural region before 2006, and has now become a low-density residential area (Fig. 9(b)). The measurement was made at a height of 9 m at the balcony of one residential building rather than at pedestrian level mainly for safety and security reasons. The station at Xietaizi is more urban and surrounded by residential buildings and lawns. The measurement height was 12 m. However, all the measurements are converted to a height of 3 m by considering the vertical temperature gradient. This is a well-known and classic method in outdoor meteorological measurement (Oke, 1988). The major measuring parameters are air temperature and relative humidity. The instrument was a ZDR automatic data logger with

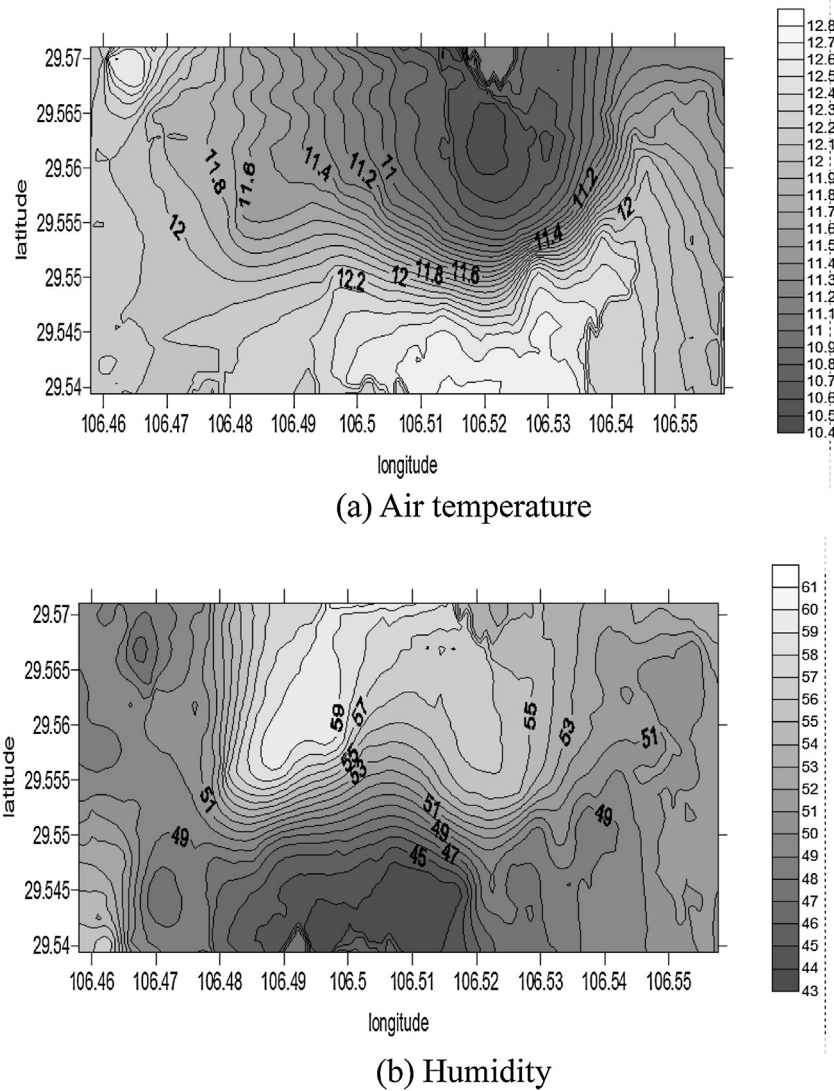


Fig. 14. Air temperature and humidity mapping for the mobile transverse route I.

the sensor inside and radiation shield outside. The data collection started in June 2012 and six months of data have been collected.

The urban heat island intensity is expressed by the difference between the urban air temperature and the rural air temperature. In the analysis, it would be:

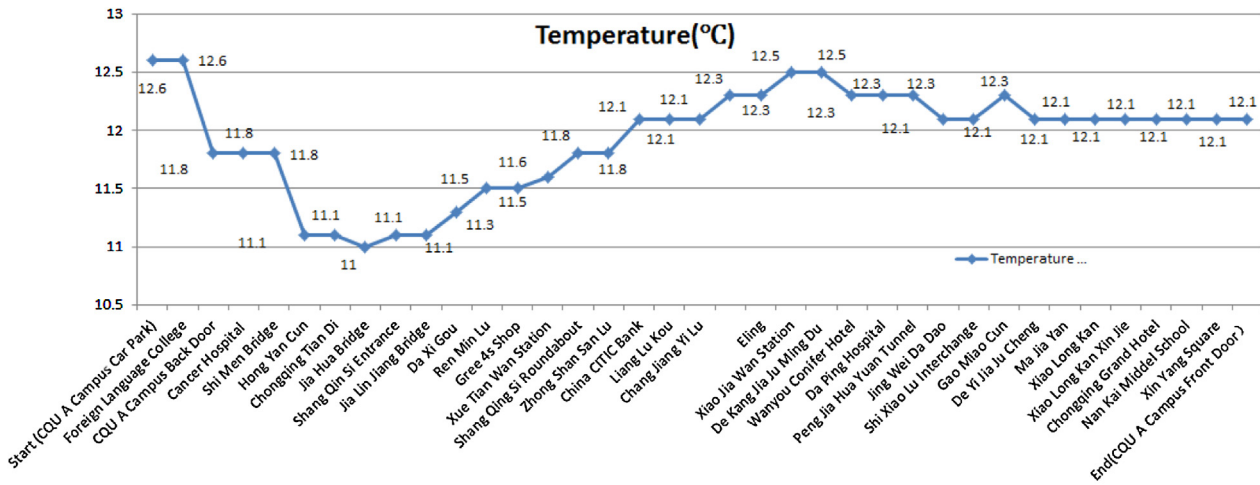
$$\Delta T = T_{\text{xietazi}} - T_{\text{huxi}}$$

The monthly averaged urban heat island intensities between the two sites from July to December were calculated and shown in Fig. 10. A typical 'U' shape is found for the diurnal pattern. An urban cool island is found around Midday, which is also found elsewhere in the world. Middel, Hüb, Brazel, Martin, and Guhathakurta (2014) found that dense urban forms can actually create local cool islands using ENVI-met simulation. Spatial differences were determined by solar radiation and local shading patterns. Chang, Li, and Chang (2007) detected that an urban park can produce a local urban cooling island, especially for parks with tall and shady trees. Therefore, the urban air temperature can be relatively lower compared with rural sites due to the shading effect of surrounding buildings or the existence of local water bodies or urban forest. The maximum urban heat island occurs at around 1:00 a.m. but the magnitude is different from month to month. A lower urban heat island intensity, i.e., smaller than 1 °C, is found during autumn (September, October

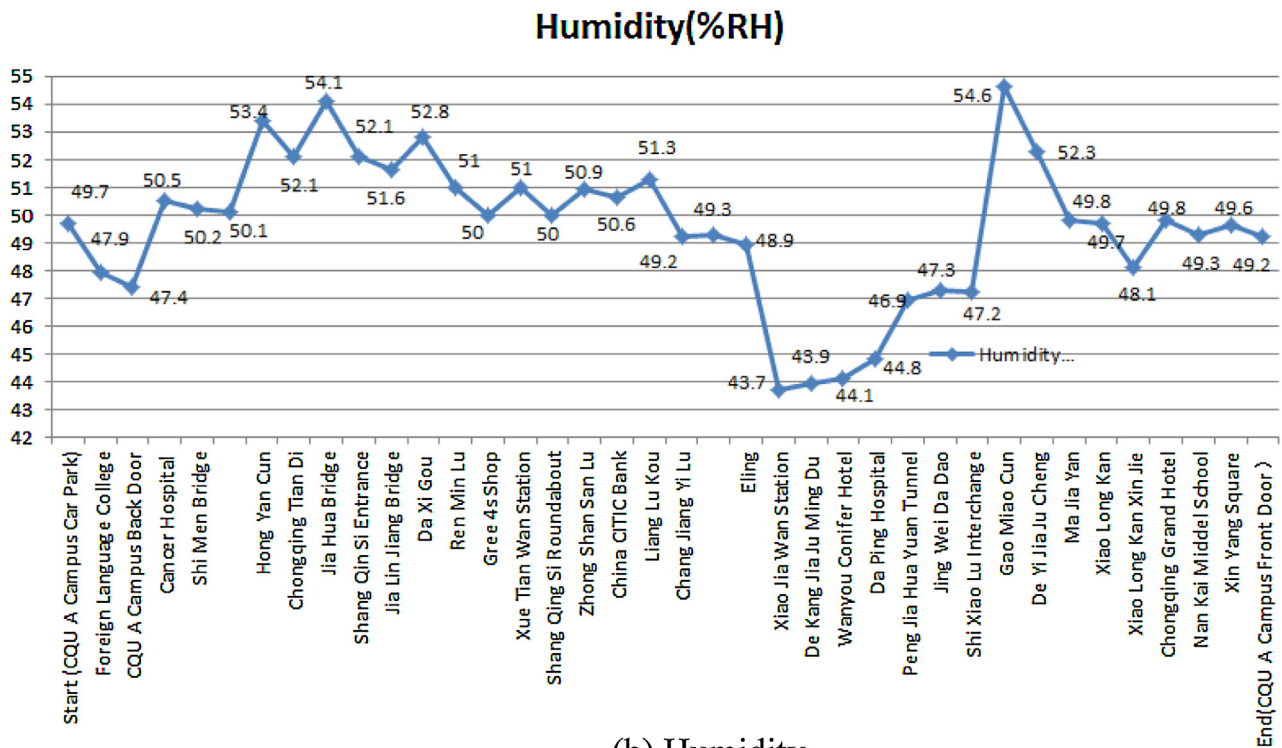
and November). However, in the summer months, such as August, the maximum heat island intensity can be as high as 2.5 °C, indicating that the urban heat island is more profound in summer in Chongqing.

3.2. Mobile transverse measurement

Mobile transverse measurement is a good way of complementing the fixed weather station measurements, as it can provide a spatial distribution. A weather station is installed on a car roof to measure air temperature and humidity at the same time when the car makes the transverse trips. The Global Positioning System (GPS) is used to record the transverse route, as shown as Fig. 11. Software Surfer version 11 (Goldensoftware, 2012) can be used for post-processing for urban heat island mapping. Several field campaigns are made. Two specific days were chosen representing two typical weather types in Chongqing: one is clear and cloudless with intense solar radiation and the other is cloudy with little solar radiation. We are interested to investigate how the landscape responds to these two distinct weather types. We chose the starting time at around 14:00 as the solar radiation is most intensive around that time. In addition, the heat and moisture transfers reach their maximum for the water bodies such as the Yangtze and Jialing Rivers



(a) Air temperature



(b) Humidity

Fig. 15. Air temperature and humidity mapping for the mobile transverse campaign II.

that play an important role in regulating the thermal environment in Chongqing. All the instruments were calibrated before and after the tests, and the data output were validated by the nearest fixed weather station.

3.2.1. Campaign 1

The transverse measurement started at 14:11:10. Dec 24, 2012 and ended at 15:17:40 Dec 24, 2012. The whole measurement took 1 h and 6 mins. The weather was clear and sunny. The air temperature, RH and location (latitude and longitude) are measured simultaneously. The sampling time is 10 s. Fig. 12 depicts the mapping of air temperature and humidity for this transverse measurement with detailed latitude and longitude information. It is evident that there is a much lower air temperature

and higher RH near the Jialing River. There are several cool islands.

Furthermore, some typical urban locations which are on the transverse route are selected to examine the relationship of air temperature and RH with the local environmental conditions including land cover, building/population density, greenery etc. As shown in Fig. 13, a relatively high temperature is expected in locations such as Changjiangyilu, Eling etc., where a dense urban morphology and little greenery are found.

3.2.2. Campaign 2

The second transverse measurement took place at 14:05:20 Jan 8, 2013, and ended at 15:02:50 the same day. The duration was 57 mins. The sky was cloudy during that period. The same

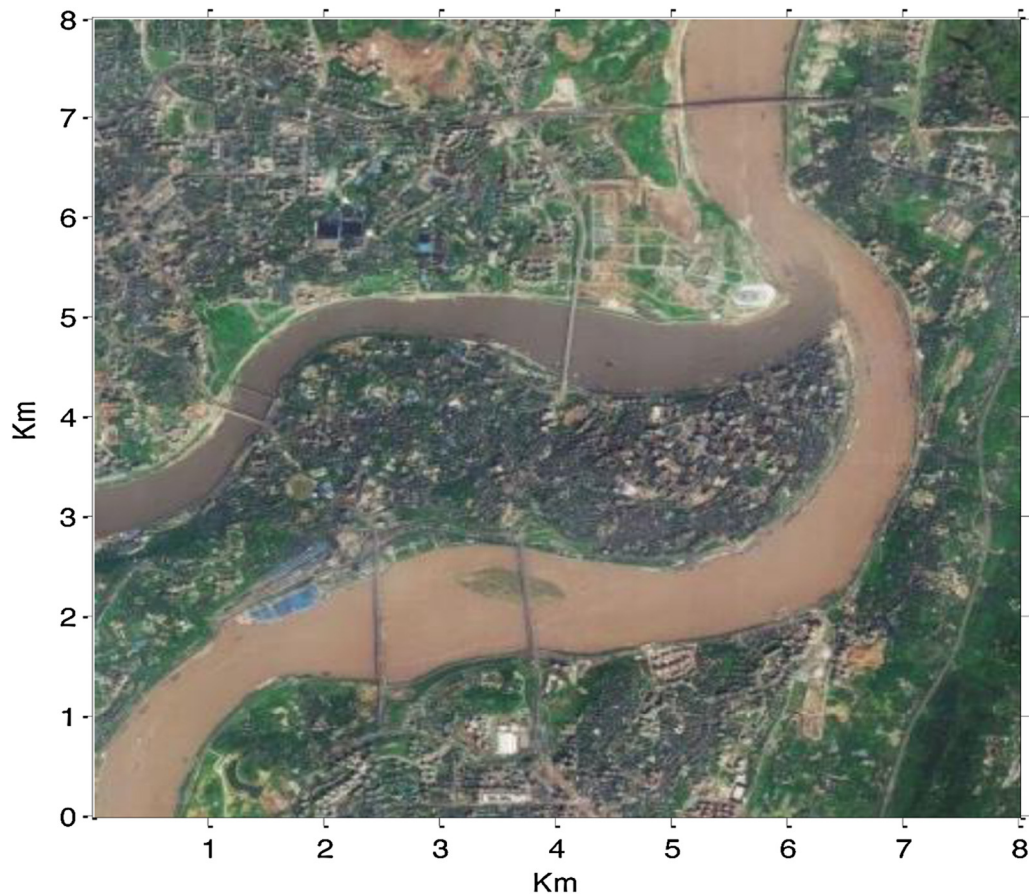


Fig. 16. Simulation domain.

transverse route was followed. The measurement results are presented in Fig. 14. As with the first campaign, it was cool and humid near the river, but in contrast with sunny and calm days in campaign 1, a much more well-defined cool and humid island was found. The temperature and relative humidity are much homogeneous for cloudy situation. This can also be reflected in Fig. 15 where the same locations are chosen as in Fig. 13. Compared with Fig. 13, it is obvious that there is much less fluctuation in terms of temperature and RH among the urban locations. This indicates that the thermal environment is more determined by large-scale meteorological forces under cloudy conditions, but during the clear and sunny days, the local heterogeneity will play an important role in the local climate.

4. Numerical simulation

Techniques for modeling urban microclimates and the temperatures of urban block surfaces are desired by urban planners and architects for the early stages of strategic urban designs. We developed a simplified mathematical model for urban simulations (UMsim) (Yao, Luo, and Li, 2011) including urban surfaces temperatures and microclimates. The nodal network model has been developed by integrating coupled thermal and airflow models. Direct solar radiation, diffuse radiation, reflected radiation, long-wave radiation, heat convection in air and heat transfer in the exterior walls and ground within the complex have been taken into account. The principle of the simplified mathematical model is to integrate the Digital Elevation Model (DEM) with the coupled thermal and airflow model in order to perform urban microclimate calculations simultaneously. The whole urban complex can be divided into a number of zones and the relevant equations for the mass, pressure and energy balance of each zone have thus been

established. The detailed illustration of the model can be found in Yao et al. (2011).

Our self-developed simulation program was applied to the thermal environment of Chongqing. Fig. 16 is the simulation domain, covering 8 km × 8 km. The numerical simulation is applied for a typical day of July in 2012 (21/7/2012). The simulation resolution level is 400 × 400, with 160,000 pixels. Each pixel represents 400 m². The attributes of urban parameters have been referred with published handbooks. The code has been tuned to meet the realistic conditions the best in order to ensure the accuracy of the model. The input parameter includes the DEM map of the studied area, hourly meteorological weather data from the weather station located in the rural area including air temperature, humidity, solar radiations (direct and horizontal diffuse) and wind speed. We carried out a survey and measurement in the selected representative area; the parameters collected include the reflectivity and emissivity of building roofs, surfaces, and pavements of the area. The weighted average reflection has been calculated using the following equation:

$$\rho_{\text{average}} = \frac{\sum_i \rho_i A_i}{\sum_i A_i}$$

where, ρ_{average} is the average reflectivity; A_i is the area of different surfaces; ρ_i is the reflectivity of different material.

The weighted average reflectivities of the building area and non-building area can be therefore calculated by substituting the values measured from the studied field. The final average reflectivity of the studied area can be determined by aggregating the calculated reflectivities of ground area, roof area and facade area.

The respective output results are surface and air temperatures at a height of 3 m. Figs. 17 and 18 show the simulation results. The

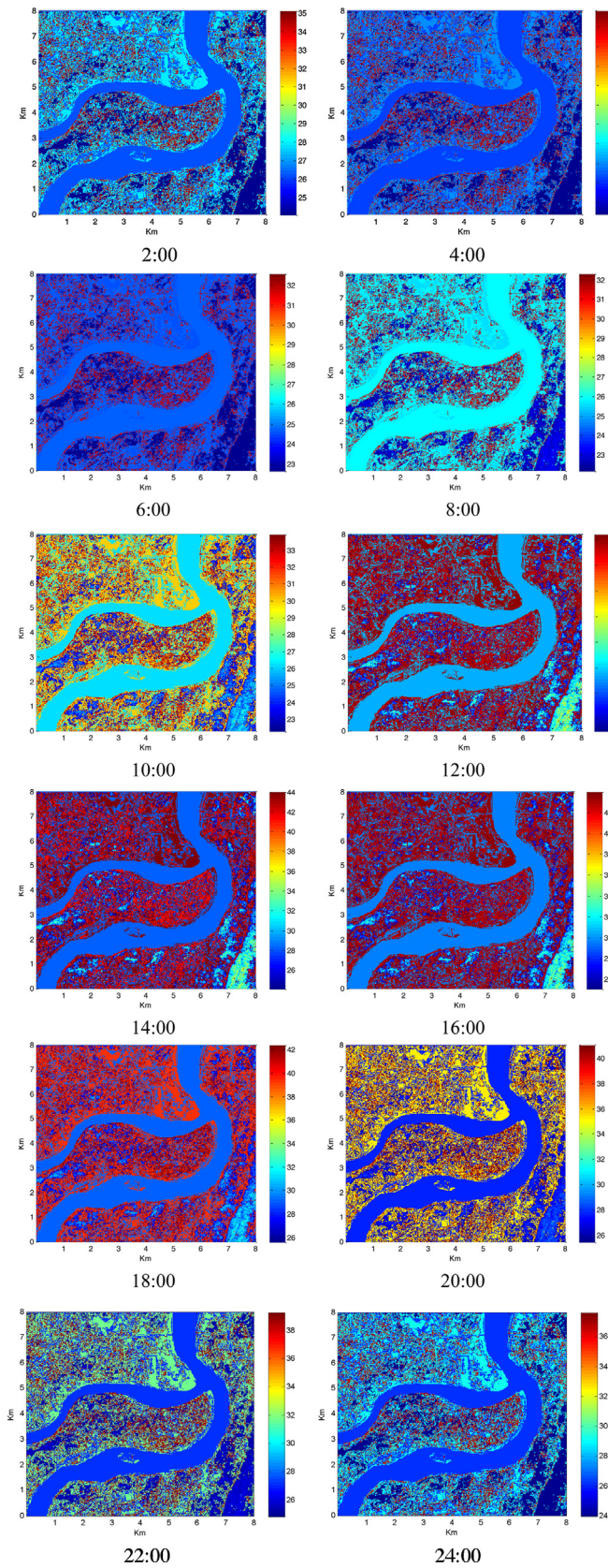


Fig. 17. Surface temperature distribution.

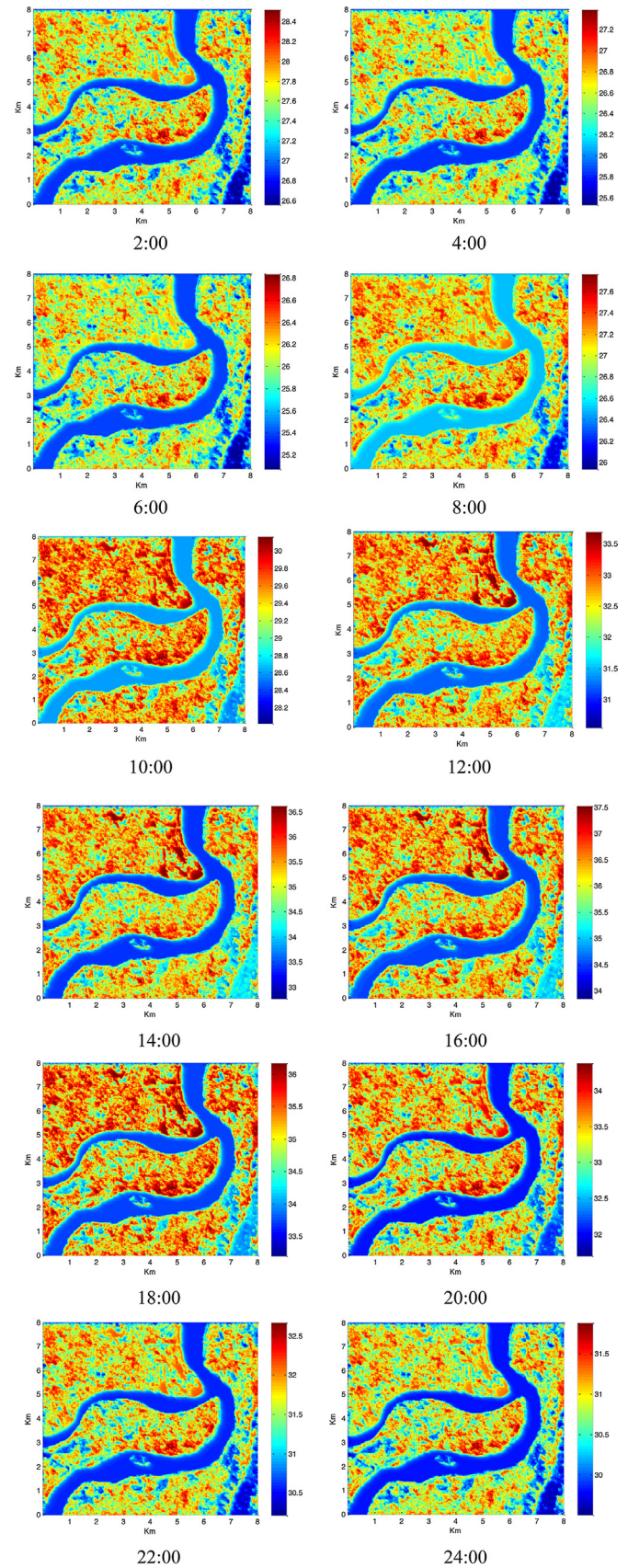


Fig. 18. Air temperature distribution at a height of 3 m.

surface temperature gradually increases since the sun starts to rise at 06:00. The urban surface receives intense solar radiation, and reaches its maximum temperature as high as 44 °C at around 14:00 due to the thermal storage effect. It then gradually decreases when the solar radiation reduces, and further decreases during the night due to the radiative loss to the sky. However, at night, the maximum temperature in the urban area can still be as high as 36 °C in some regions, indicating a significant surface urban heat island phenomenon in Chongqing. The surface temperature reaches its minimum at around 06:00 just before sunrise. Spatially, the water temperature of the river is always lower than that of the urban surface, but there is a significant diversity within the urban areas. Some cooling spots are observed within the urban districts, which is in accordance with the presence of urban greenery.

In terms of the air temperature distribution, quite similar patterns with surface temperature are found. The air is first heated up in the morning by the sun, and the temperature gradually increases due to the convective heat transported by the heated surface. The air temperature reaches its maximum at around 16:00 which is later than the surface temperature. It is still very hot during the summer night time, the maximum air temperature can be as high as 34 °C. In some regions within the urban area, such as a park or lawn, a lower temperature is expected. Under the cooling impact of the river, a lower air temperature is found near the river, which is consistent with our findings from the field campaign. The cooling effect of the water body within the city can never be ignored. Moreover, the highest temperature always corresponds with the highest population and building density.

5. Concluding remarks and future outlook

This paper investigated the urban microclimate in Chongqing by examining relevant Chinese and English publications, undertaking field experimental campaigns and creating a numerical simulation against the background of the rapid urbanization in Chongqing. The comprehensive literature review of current Chinese publications strongly suggests that a further study on this topic is needed. Therefore, two types of field measurement campaigns were carried out: fixed-station measurement and mobile transverse measurement. For the urban surface/air temperature, an in-house-developed program is used to simulate the urban thermal environment in Chongqing. This provides a better tool for urban planners to study the effects of different urban planning scenarios. The major conclusions drawn from this project are:

- An average rising trend of 0.10 °C/decade was found for the annual mean temperature from 1951 to 2010 in Chongqing. This number is much higher than the global rising trend of 0.074 °C/decade, indicating a higher degree of urban warming in Chongqing. Especially, a much more significant increasing trend of urban air temperature is observed since 1980 which is associated with the ongoing unprecedented urbanization in Chongqing.
- The urban microclimate is very sensitive to the local environment. A higher air temperature is always related to a higher building density and population density.
- The urban heat island intensity in Chongqing is stronger in summer compared to autumn and winter. The maximum urban heat island intensity occurs at around 24:00 and can be as high as 2.5 °C. In the daytime, an urban cool island exists.
- The mobile measurements show that the local greenery has a great impact on the local thermal environment. Urban green spaces can help to reduce urban air temperature and therefore mitigate urban heat islands.
- The cooling effect of an urban river is limited in Chongqing, as both sides of the river are the most developed areas, but the

relative humidity is much higher near the river compared with more distant locations.

- Numerical simulation combined with digital elevation mapping is powerful in predicting the urban air temperature on an urban micro-scale. The predicted results agree with the onsite and mobile measurements. The urban air/surface temperature is very sensitive to the local land cover and anthropogenic activities. Also, urban heat storage plays an important role in determining the urban temperature. The urban fabric stores the heat and releases it later, which creates a profound urban heat island at night.
- The on-site survey and measurement of the reflectivities of the surfaces of building and ground involves large amount of work but significantly improve the accuracy of the simulation. When the work of survey and measurement is not available, typical urban thermal properties could be referred with little significant compromise of accuracy.

Attempts have been made to contribute to the understanding of the urban thermal environment in Chongqing, but it is still subject to some limitations. For example, the coverage of the mobile transverse trips is limited; the weather station network is far more complete. The numerical simulation does not take into account the surrounding topography which is a unique geographical feature of Chongqing. Moreover, the effect of the TGR on the surrounding environment is very complicated and impossible to fully address in a single project. More research toward a better understanding of the urban thermal environment in Chongqing is needed.

Acknowledgements

The Authors would like to thank the financial support from the RICS Research Trust (2012). The urban microclimate simulation tool was financially supported by the UK Engineering Physical and Science Research Council (EPSRC EP/F039867/1) and the National Natural Science Foundation of China (51178481; 50808182).

References

- Ash, C., Jasny, B. R., Roberts, L., Stone, R., & Sugden, A. M. (2008). *Reimagining cities*. *Science*, 319, 739.
- Belcher, S. E. (2005). *Mixing and transport in urban areas*. *Philosophical Transactions of the Royal Society A: Mathematical, Physical and Engineering Sciences*, 363, 2947–2968.
- Bornstein, R. D. (1968). *Observations of the urban heat island effect in New York City*. *Journal of Applied Meteorology*, 7, 575–582.
- Bowler, D. E., Buyung-Ali, L., Knight, T. M., & Pullin, A. S. (2010). *Urban greening to cool towns and cities: A systematic review of the empirical evidence*. *Landscape and Urban Planning*, 97, 147–155.
- Busato, F., Lazzarin, R. M., & Noro, M. (2014). *Three years of study of the Urban Heat Island in Padua: Experimental results*. *Sustainable Cities and Society*, 10, 251–258.
- Chang, C.-R., Li, M.-H., & Chang, S.-D. (2007). *A preliminary study on the local cool-island intensity of Taipei city parks*. *Landscape and Urban Planning*, 80(4), 386–395.
- Chongqing Bureau. (2011). *Chongqing Statistical Yearbook 2011*. (in Chinese).
- Grimmond, S. (2007). *Urbanization and global environmental change: Local effects of urban warming*. *Geographical Journal*, 173, 83–88.
- Goldensoftware. (2012). *Surfer 11*. <http://www.goldensoftware.com/products/surfer>
- Howard, L. (1833). *The climate of London*. London.
- Huang, L., Li, J., Zhao, D., & Zhu, J. (2008). *A fieldwork study on the diurnal changes of urban microclimate in four types of ground cover and urban heat island of Nanjing, China*. *Building and Environment*, 43(1), 7–17.
- IPCC. (2007). *Fourth Assessment Report: Climate change 2007*.
- Kruger, A. C., & Shongwe, S. (2004). *Temperature trends in South Africa: 1960–2003*. *International Journal of Climatology*, 24, 1929–1945.
- Li, Y., Geng, D., Dong, X., & Zhu, Y. (2010). *Climate change of wind speed in Chongqing from 1961 to 2007*. *Transactions of Atmospheric Sciences*, 33, 4 (in Chinese).
- Middel, A., Häb, K., Brazel, A. J., Martin, C. A., & Guhathakurta, S. (2014). *Impact of urban form and design on mid-afternoon microclimate in Phoenix Local Climate Zones*. *Landscape and Urban Planning*, 122, 16–28.
- Mills, G. (2007). *Cities as agents of global change*. *International Journal of Climatology*, 7, 1849–1857.

- Mölders, N., & Olson, M. A. (2004). Impact of urban effects on precipitation in high latitudes. *Journal of Hydrometeorology*, 5, 409–429.
- Nations Union. (2005). *World urbanization prospects: The 2005 revision*. New York: Department of Econ and Social Affairs, Population Division. <http://www.un.org/esa/population/publications/WUP2005/2005WUPHighlights.Exec.Sumpdf>. Accessed 18.06.13
- Normile, D. (2008). China's living laboratory in urbanization. *Science*, 319, 740–743.
- Oke, T. R. (1988). *Boundary layer climate* (2nd ed.). Routledge.
- Papanastasiou, D., & Kittas, C. (2012). Maximum urban heat island intensity in a medium-sized coastal Mediterranean city. *Theoretical Applied Climatology*, 107, 407–416.
- Robaa, S. M. (2013). Some aspects of the urban climates of Greater Cairo Region, Egypt. *International Journal of Climatology*, 33, 3206–3212.
- Si, P., Ren, Y., Liang, D., & Lin, B. (2012). The combined influence of background climate and urbanization on the regional warming in Southeast China. *Journal of Geographical Sciences*, 22, 245–260.
- Wu, H., Ye, L.-P., Shi, W.-Z., & Clarke, K. C. (2014). Assessing the effects of land use spatial structure on urban heat islands using HJ-1B remote sensing imagery in Wuhan, China. *International Journal of Applied Earth Observation and Geoinformation*, 32(0), 67–78.
- Wu, L., Zhang, Q., & Jiang, Z. (2006). Three Gorges Dam affects regional precipitation. *Geophysical Research Letters*, 33, L13806.
- Wong, N. H., & Yu, C. (2005). Study of green areas and urban heat island in a tropical city. *Habitat International*, 22, 547–558.
- Yang, F., Lau, S. S. Y., & Qian, F. (2010). Summertime heat island intensities in three high-rise housing quarters in inner-city Shanghai China: Building layout, density and greenery. *Building and Environment*, 45(1), 115–134.
- Yao, R., Luo, Q., & Li, B. (2011). A simplified mathematical model for urban microclimate simulation. *Building and Environment*, 46, 253–265.
- Zeng, Y., Qiu, X. F., Gu, L. H., He, Y. J., & Wang, K. F. (2009). The urban heat island in Nanjing. *Quaternary International*, 208(1–2), 38–43.
- Zhang, H., Qi, Z., Ye, X., Cai, Y., Ma, W., & Chen, M. (2013). Analysis of land use/land cover change, population shift, and their effects on spatiotemporal patterns of urban heat islands in metropolitan Shanghai, China. *Applied Geography*, 44(0), 121–133.
- Zhang, T., Cheng, B., & Liu, X. (2009). Climate change and scientific solutions in Chongqing. *China Venture Capital* (in Chinese).
- Zhao, W., Sun, W., & Cheng, B. (2008). Analysis of the temperature variations and their reasons in Sichuan and Chongqing. *Plateau and Mountain Meteorology Research*, 28, 9 (in Chinese).